Modeling Transcranial Electric Stimulation in Mouse: A High Resolution Finite Element Study

John M. Bernabei*, Won Hee Lee*, *Student Member, IEEE*, and Angel V. Peterchev, *Member, IEEE*

***Abstract*— Mouse models are widely used in studies of various forms of transcranial electric stimulation (TES). However, there is limited knowledge of the electric field distribution induced by TES in mice, and computational models to estimate this distribution are lacking. This study examines the electric field and current density distribution in the mouse brain induced by TES. We created a high-resolution finite element mouse model incorporating ear clip electrodes commonly used in mouse TES to study, for example, electroconvulsive therapy (ECT). The electric field strength and current density induced by an ear clip electrode configuration were computed in the anatomically realistic, inhomogenous mouse model. The results show that the median electric field strength induced in the brain at 1 mA of stimulus current is 5.57 V/m, and the strongest field of 20.19 V/m was observed in the cerebellum. Therefore, to match the median electric field in human ECT at 800 mA current, the electrode current in mouse should be set to approximately 15 mA. However, the location of the strongest electric field in posterior brain regions in the mouse does not model well human ECT which targets more frontal regions. Therefore, the ear clip electrode configuration may not be a good model of human ECT. Using high-resolution realistic models for simulating TES in mice may guide the establishment of appropriate stimulation parameters for future *in vivo* studies.**

I. Introduction

TRANSCRANIAL electric stimulation (TES) paradigms—including electroconvulsive therapy (ECT), transcranial direct current stimulation, transcranial alternating current stimulation, and others—achieve neuromodulatory effects by stimulating the brain with electric current delivered by electrodes placed on the scalp. Electroconvulsive therapy (ECT), the most widely used form of TES, is currently the most effective treatment for major depression [1]. In TES, as current flows through the scalp, skull, and cerebrospinal fluid (CSF) before entering the brain, the induced electric field depends upon the geometries and conductivities of the biological structures present in the subject [2]–[4]. In order to understand the biophysical effects of TES, a computational model is valuable for optimizing TES techniques and can be used to estimate the induced electric field strength and distribution in the brain as a result of stimulation.

TES techniques have been widely applied to mouse models *in vivo*. For example, *in vivo* mouse TES models have been used to study cortico-cortical connections, immunoreactivity in hippocampus and hypothalamus, motor excitation, effects of antiepileptic drugs, as well as epigenetic changes resulting from brain stimulation [5]-[9]. Therefore, in order to interpret and optimize mouse TES studies as well as to compare and match dosing between mouse and human paradigms studies, there is a need for computational models that predict the strength and distribution of the electric field during TES in mice.

Finite element models have been previously used to investigate the effects of other brain stimulation paradigms in rodents. Gasca et al. used a finite element model to investigate the electric field resulting from transcranial current stimulation in rats [10]. Salvador et al. created a finite element model to simulate transcranial magnetic stimulation in mice [11]. Despite these efforts, there has not been a model to compute the biophysical effects of TES in mice using a realistic high-resolution geometry.

One of the most common electrode montages used in mice is the ear clip configuration [12], preferred for its relative ease of application. However, since this paradigm is not commonly used in humans, and due to the vast anatomical differences between mice and humans, the resulting electric field and how it differs from human stimulation paradigms are unknown.

In this paper, we present a realistic, whole-body, inhomogeneous, high-resolution finite element mouse model incorporating ear clip electrodes commonly used in rodent TES. We simulate the electric field strength and current density induced by this TES configuration, and examine their characteristics including overall strength and distribution in the brain. This study demonstrates the utility of realistic computational models to guide optimal stimulation parameters for future mouse TES studies, and may offer insight into how well these experiments mimic human TES.

II. Methods

A. High-resolution Finite Element Model Generation

An anatomically realistic finite element mouse model was derived from computed tomography (CT) data. The labeled atlas data of a nude normal male mouse was acquired from the Biomedical Imaging Group at University of Southern California, http://neuroimage.usc.edu/Digimouse.html [13], [14].

This work was supported in part by NIH grant R01MH091083. *These authors contributed equally to this work.

J. M. Bernabei is with the Department of Biomedical Engineering, Duke University, Durham, NC 27710, USA (e-mail: john.bernabei@duke.edu).

W. H. Lee is with the Department of Biomedical Engineering, Columbia University, New York, NY 10027 and with the Department of Psychiatry and Behavioral Sciences, Duke University, Durham, NC 27710, USA (e-mail: wl2324@columbia.edu).

A. V. Peterchev is with Departments of Psychiatry and Behavioral Sciences, Biomedical Engineering, and Electrical and Computer Engineering, Duke University, Durham, NC 27710, USA (phone: 919-684-0383; fax: 919-681-9962; e-mail: angel.peterchev@duke.edu).

978-1-4244-7929-0/14/$26.00 ©2014 IEEE

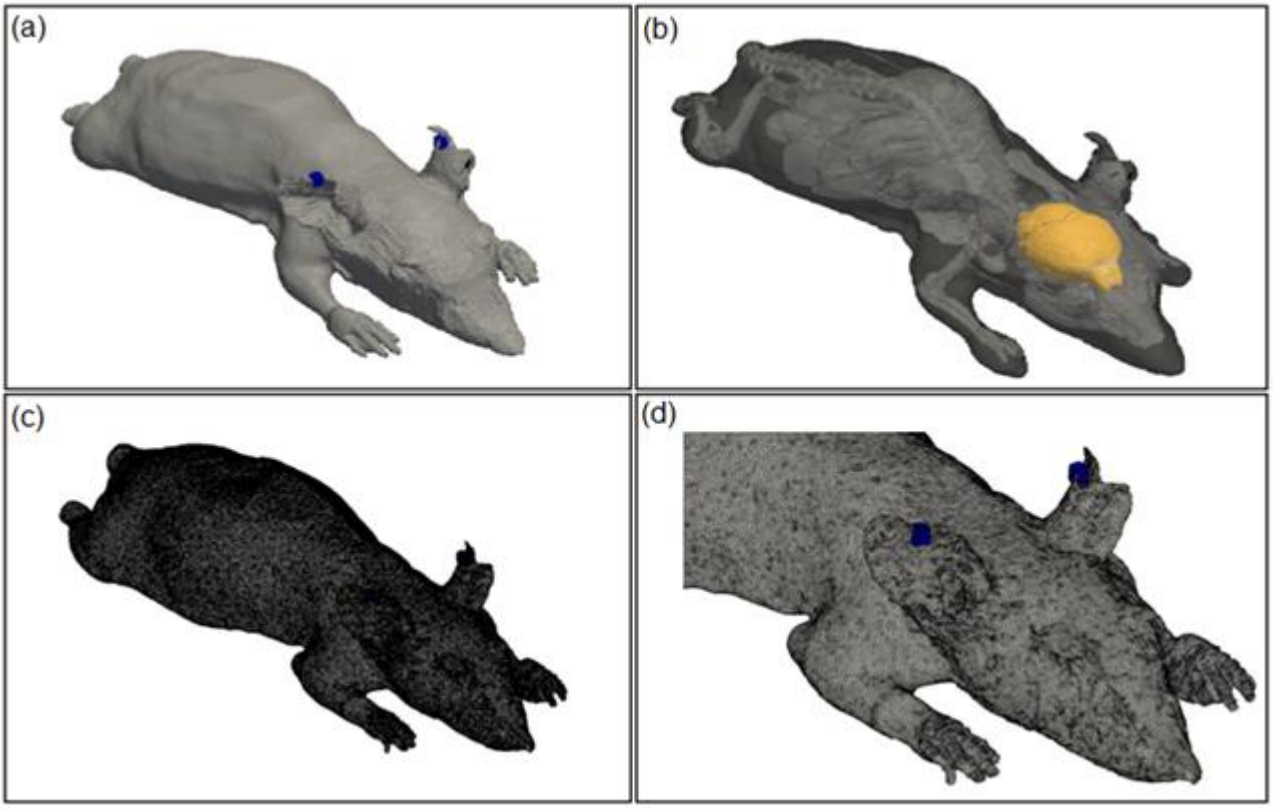

Fig. 1. (a) Three dimensional rendering of the mouse model with the ear clip electrodes highlighted in blue. (b) Three dimensional rendering of the mouse with transparent skin, showing the internal structures including the brain which is highlighted in yellow. (c) The full finite element mesh with approximately 2 million elements. (d) The front half of the finite element mesh with the ear clip electrodes in blue.

The whole body mouse atlas data included 21 tissue segmentation regions with cubic voxel size of 0.1 mm and a matrix dimension of 380×992×208. We further refined this segmentation atlas using manual segmentation editing tools in the ITK-SNAP software [15]. Specifically, we included a layer of highly conductive CSF, ears, as well as air-filled sinuses based on the provided CT data and cryosection data from the Biomedical Imaging Group at the University of Southern California, and the Golgi atlas of the postnatal mouse brain [16]. We also modeled the two clip electrodes and positioned them on each ear as commonly used in rodent TES studies (see Fig. 1). The complete mouse whole-body model incorporating the TES electrodes was adaptively meshed using the restricted Delaunay triangulation algorithm [17], [18], resulting in a finite element model of the whole mouse body and electrodes consisting of approximately 2 million tetrahedral elements.

B. Electric Field Simulation

The finite element mouse model was imported into COMSOL Multiphysics (COMSOL Inc., Burlington, MA, USA). We acquired the electric field solutions by solving the quasi-static Laplace equation

$$\nabla \cdot (\sigma \nabla V) = 0 \qquad (1)$$

where V and σ denote the electric potential and tissue electrical conductivity, respectively.

All tissue compartments were treated as isotropic. The isotropic conductivity values were assigned as given in Table I [19]. One electrode in the model was assigned to ground potential, and the other was assigned a fixed voltage relative to ground. The normal current density was integrated over a saggital plane between the electrodes to calculate the total electrode current, and the voltage between the electrodes was scaled to inject a total current of 1 mA. The linear equation system of the finite element method was solved using the Multifrontal Massively Parallel Sparse Direct Solver (MUMPS) within COMSOL. Solving the model which contained approximately 3 million degrees of freedom took under 30 minutes on a computer with 16 GB RAM and a 4 core 3.4 GHz processor.

TABLE I
TISSUE ELECTRICAL CONDUCTIVITIES (S/M)

Tissue	Conductivity
Soft tissue	0.33
Bone	0.0083
Cerebrospinal fluid	1.79
Brain	0.33
Eye	0.5
Air	0
Steel Electrode	9.8×10^5

III. RESULTS

Fig. 1 shows 3-D renderings as well as finite element meshes of the mouse model depicting the location of electrodes, the detail of exterior and interior structures, as well as

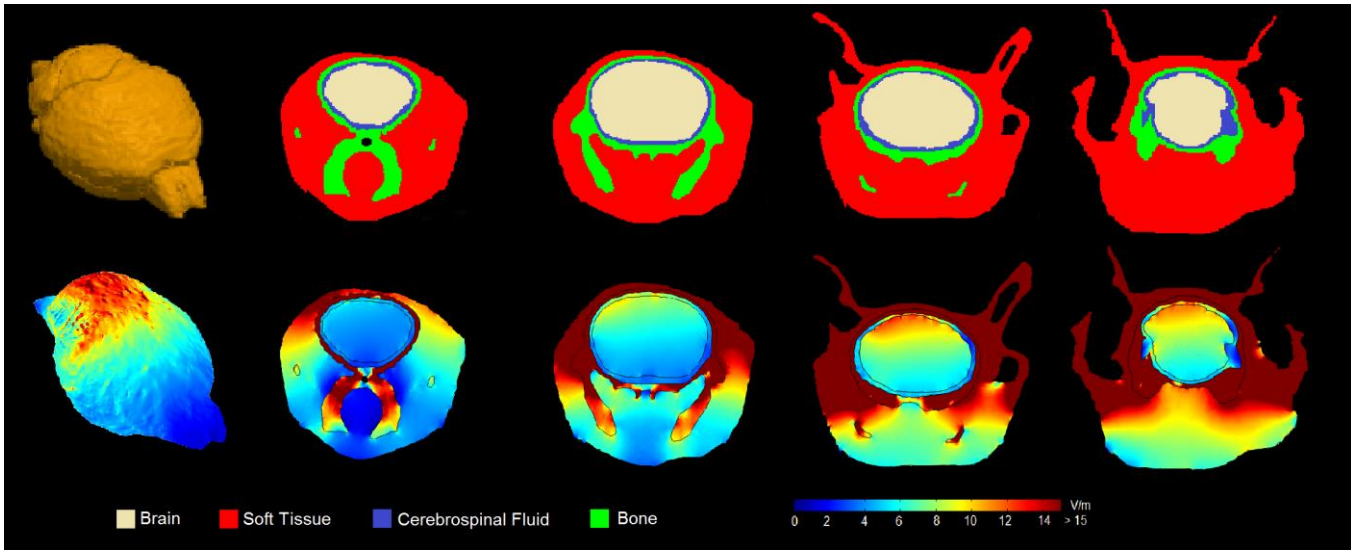

Fig. 2. Left column: 3-D rendering of the mouse brain with corresponding surface electric field map. Right: four coronal slices of the mouse head segmentation (top) with their corresponding electric field distributions (bottom).

the high density of the mesh.

Fig. 2 shows a 3-D rendering of the mouse brain and its corresponding electric field map, as well as four evenly spaced coronal slices of both the tissue segmentation as well as the electric field distributions calculated for these slices. The slices were taken at 17.5, 20, 22.5, and 25 mm from the tip of the nose of the mouse model. As expected, the electric field in the scalp overlaying the skull is strongest due to the high electrical impedance of the skull. The electric field is strongest in superior and posterior regions of the brain. Specifically, the strongest electric field appears on the dorsal surface of the posterior cerebrum and the cerebellum.

Fig. 3 shows a histogram depicting the distribution of electric field strengths across the nodes in the model of the mouse brain. Table II gives a summary of the electric field and current density values occurring in the mouse brain for 1 mA of stimulating current.

Fig. 4 compares regions outside the cerebellum with the electric fields in the cerebellum. As expected from the electric field maps in Fig. 2, the cerebellum experienced a higher electric field strength than the rest of the brain, with a median value of 8.38 V/m compared to 5.03 V/m, respectively. Additionally, the highest electric field strength experienced by the mouse brain was 20.2 V/m, occurring in the cerebellum.

TABLE II
ELECTRIC FIELD STRENGTH AND CURRENT DENSITY IN MOUSE BRAIN AT 1 MA STIMULUS CURRENT

Statistic	Electric Field Strength (V/m)	Current Density (A/m^2)
Median	5.57	1.99
Mean	6.02	1.83
Standard Deviation	2.78	0.92

IV. DISCUSSION

We described the creation of a high-resolution finite element model of a mouse and its use to simulate the electric field distributions in the mouse brain generated by TES with an ear clip electrode montage. The model allows the estimation of the electric field direction and magnitude per unit electrode current in various brain regions. For example, this computational model can be used to determine approximate parameters for rodent ECT by scaling stimulation currents to match the strength of the induced electric field in human ECT. For stimulation current of 800 mA conventionally used in clinical ECT, bilateral ECT induces a median electric field of 85 V/m in the human brain [20]. Using the median electric field of 5.57 V/m for 1 mA current reported in this study, electrode current of 15.3 mA would be necessary to induce comparable electric field magnitude in the mouse brain as in the human brain. This estimate is close to the current strength (18–25 mA) used in *in vivo* electroconvulsive shock studies in mice [9], [6].

Importantly, however, for appropriate modeling of human ECT in a mouse model, not only the overall electric field strength, but also the electric field spatial distribution should be approximated. This is because the therapeutic efficacy as well as side effects of ECT are highly dependent on the electrode placement, in addition to the stimulus current parameters [21]. Our mouse simulation showed that the electric field is strongest towards the midbrain, and in the cerebellum. The cerebellum is not a known target for ECT in humans; rather human ECT targets more frontal brain structures [16]. Therefore, the ear clip electrode configuration in mouse, inducing strongest electric field in posterior-superior brain regions including the cerebellum, may not be an accurate model for human ECT.

A limitation of this model is that the brain was approximated as a homogeneous conductor with an isotropic conductivity of 0.33 S/m. As different regions in the brain have different conductivities (e.g. gray matter and white matter), a more detailed brain segmentation could be useful for increasing the accuracy of the results.

In conclusion, the high-resolution finite element mouse model presented in this study provides a useful method for investigating the biophysical effects of various TES para-

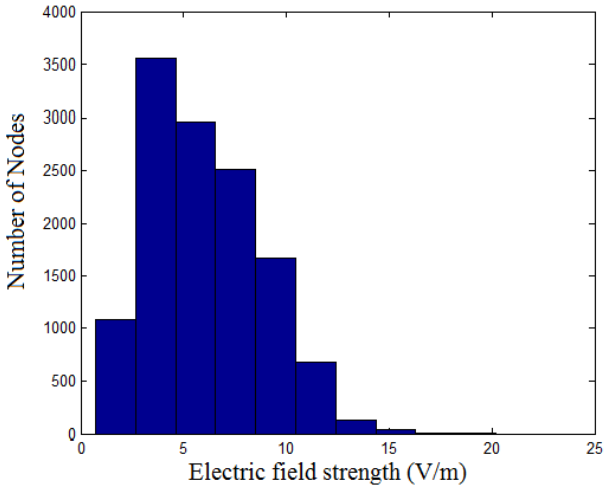

Fig. 3. Histogram of the electric field magnitude at the finite element mesh nodes comprising the mouse brain at 1 mA stimulus current.

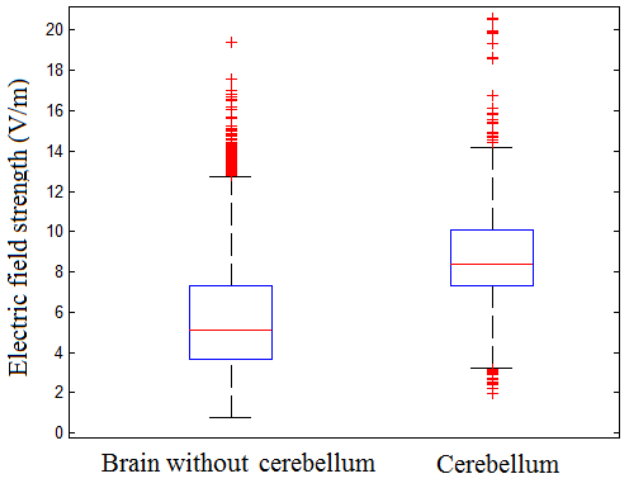

Fig. 4. Comparison of the electric field magnitude in the whole brain without the cerebellum and in the cerebellum at 1 mA stimulus current.

digms, including ECT. The stimulus current for an ear-clip electrode montage should be set to ~15 mA to approximate the overall stimulation strength of human ECT. However, the strongest electric field was induced in the midbrain and cerebellum of the mouse. Thus, the ear clip electrode montage in mice may not be a good model of human ECT which conventionally targets more frontal regions.

V. Acknowledgement

The authors thank Dr. Zhi-De Deng and Walter Barnes for their helpful comments and suggestions.

VI. References

[1] R. Abrams, Electroconvulsive Therapy, 4th Ed. New York: Oxford University Press, 2002.

[2] Z. D. Deng, S. H. Lisanby, and A. V. Peterchev, "Effect of anatomical variability on neural stimulation strength and focality in electroconvulsive therapy (ECT) and magnetic seizure therapy (MST)," *Conf. Proc. IEEE Eng. Med. Biol. Soc.,* pp. 682-688, 2009.

[3] W. H. Lee, S. H. Lisanby, A. F. Laine, and A. V. Peterchev, "Stimulaton strength and focality of electroconvulsive therapy with individualized current amplitude: a preclinical study," *Conf. Proc. IEEE Eng. Med. Biol. Soc.,* pp. 6430-6433, 2012.

[4] Z. D. Deng, S. H. Lisanby, and A. V. Peterchev, "Electric field strength and focality in electroconvulsive therapy and magnetic seizure therapy: a finite element simulation study," *J. Neural Eng.,* 2011.

[5] R. Hishida, K. Watanabe, M. Kudoh, and K. Shibuki, "Transcranial electric stimulation of cortico-cortical connections in anesthetized mice," *Journal of Neuroscience Methods*, vol. 201, pp. 315-321, 2011.

[6] S. Chung, H. J. Kim, I. S. Yoon, H. J. Kim, S. H. Choi, Y. S. Kim, K. H. Shin. "Electroconvulsive shock increases SIRT1 immunoreactivity in the mouse hippocampus and hypothalamus," *J. ECT.* vol. 2 pp. 93-100, 2013.

[7] M. Cambiaghi, S. Velikova, J. J. Gonzalez-Rosa, M. Cursi, G. Comi, and L. Leocani, "Brain transcranial direct current stimulation modulates motor excitability in mice," *European Journal of Neuroscience*, vol. 31, pp. 704-709, 2010.

[8] W. Loscher, "Critical review of current animal models of seizures and epilepsy used in the discovery and development of new antiepileptic drugs," *Epilepsy*, vol. 20 pp. 359-368, 2011.

[9] J. U. Guo, D. K. Ma, H. Mo, M. P. Ball, M. H. Jang, M. A. Bonaguidi, J. A. Balazer, H. I. Eaves.B. Xie, E. Ford, K. Zhang, G. L. Ming, Y. Gao, H. Song, "Neuronal activity modifies the DNA methylation landscape in the adult brain," *Nat. Neurosci.,* 2011.

[10] F. Gasca, L. Marshall, S. Binder, A. Schlaefer, U. G. Hoffman, A. Schweikard, "Finite element simulation of transcranial current stimulation in realistic rat head model", *Conf. Proc. IEEE Eng. Med. Biol. Soc.,* 2011.

[11] R. Salvador, P. C. Miranda, "Transcranial magnetic stimulation of small animals: a modeling study on the influence of coil geometry, size, and orientation," *Conf. Proc. IEEE Eng. Med. Biol. Soc.,* 2009.

[12] M. M. Castel-Branco, G. L. Alves, I. V. Figueiredo, A. C. Falcao, and M. M. Caramona, "The maximal electroshock seizure (MES) model in the preclinical assessment of potential new antiepileptic drugs," *Methods Find. Exp. Clin. Pharmacol*., 2009.

[13] D. Stout, P. Chow, R. Silverman, R. M. Leahy, X. Lewis, S. Gambhir, A. Chatziioannou, "Creating a whole body digital mouse atlas with PET, CT and cryosection images", *Molecular Imaging and Biology*, 2002.

[14] B. Dogdas, D. Stout, A. Chatziioannou, R. Leahy, "Digimouse: A 3D whole body mouse atlas from CT and cryosection data, " *Phys. Med. Bio.*, pp. 577-587, 2007.

[15] P. Yuskevich, J. Piven, H. Hazlett, R. Smith, S. Ho, J. Gee, and G. Gerig, "User-guided 3D active contour segmentation of anatomical structures: Significantly improved efficiency and reliability," *NeuroImage*, pp. 1116-1128, 2006.

[16] F. Valverde, Golgi Atlas of the Postnatal Mouse Brain, 1st Ed. New York: Springer Medicine, 2011.

[17] W. H. Lee, Z. D. Deng, T. S. Kim, A. F. Laine, S. H. Lisanby, and A. V. Peterchev, "Regional electric field induced by electroconvulsive therapy in a realistic finite element head model: influence of white matter anisotropic conductivity," *NeuroImage,* vol. 59, pp. 2110-2123, 2012.

[18] J. P. Pons, E. Segonne, J. D. Boissonnat, L. Rineau, M. Yvinec, and R. Keriven, "High-quality consistent meshing of multi-label datasets," *Inf. Process. Med. Imaging,* vol. 20, pp. 198-210,

[19] W. H. Lee, S. H. Lisanby, A. F. Laine, and A. V. Peterchev, "Anatomical variability predicts individual differences in transcranial electric stimulation motor threshold," *Conf. Proc. IEEE Eng. Med. Biol. Soc.,* pp. 815-818, 2013.

[20] Lee, W. H., Lisanby, S. H., Laine, A. F., and Peterchev, A. V. "Stimulation Strength and Focality of Electroconvulsive Therapy and Magnetic Seizure Therapy in a Realistic Head Model," *Conf. Proc. IEEE Eng. Med. Biol. Soc.*, 2014 (submitted).

[21] A. V. Peterchev, M. A. Rosa, Z. D. Deng, J. Prudic, and S. H. Lisanby, "Electroconvulsive therapy stimulus parameters: rethinking dosage," *J ECT,* 2010.